

Review Article

Modelling of Heat Transfer Phenomena for Vertical and Horizontal Configurations of In-Pool Condensers and Comparison with Experimental Findings

Davide Papini and Antonio Cammi

Department of Energy, CeSNEF-Nuclear Engineering Division, Politecnico di Milano, Via La Masa, 34, 20156 Milano, Italy

Correspondence should be addressed to Davide Papini, davide.papini@mail.polimi.it

Received 30 April 2009; Revised 30 September 2009; Accepted 28 December 2009

Academic Editor: Dubravko Pevec

Copyright © 2010 D. Papini and A. Cammi. This is an open access article distributed under the Creative Commons Attribution License, which permits unrestricted use, distribution, and reproduction in any medium, provided the original work is properly cited.

Decay Heat Removal (DHR) is a fundamental safety function which is often accomplished in the advanced LWRs relying on natural phenomena. A typical passive DHR system is the two-phase flow, natural circulation, closed loop system, where heat is removed by means of a steam generator or heat exchanger, a condenser, and a pool. Different condenser tube arrangements have been developed for applications to the next generation NPPs. The two most used configurations, namely, horizontal and vertical tube condensers, are thoroughly investigated in this paper. Several thermal-hydraulic features were explored, being the analysis mainly devoted to the description of the best-estimate correlations and models for heat transfer coefficient prediction. In spite of a more critical behaviour concerning thermal expansion issues, vertical tube condensers offer remarkably better thermal-hydraulic performances. An experimental validation of the vertical tube correlations is provided by PERSEO facility (SIET labs, Piacenza), showing a fairly good agreement.

1. Introduction

Nuclear advanced water reactor design is primarily focused on the achieving of innovative safety characteristics. The main goal of a safety design is to establish and maintain core cooling and ensure containment integrity for any transient situation, thus to minimize core damage and fission product release probabilities. The adoption of an integral layout, where the vessel hosts all the principal components of the primary circuit (reactor core, cooling pumps, steam generators, pressurizer, etc.), addresses a safety-by-design approach which increases the reactor safety.

Another important strategy in an advanced safety concept is the large utilization of passive systems, characterized by their full reliance upon natural laws (e.g., gravity and natural circulation) to accomplish their designated safety functions. Components and systems are called passive when they do not need any external input to operate. AC power sources as well as manual initiations are excluded, being the presence of moving mechanical parts and energized

actuation valves limited according to the passivity level category [1].

A typical passive safety system is the natural circulation loop able to transfer core decay heat and sensible heat from the reactor coolant to the environment during transients, accidents or whenever the normal heat removal paths are lost. Such a system consists usually of a steam generator (providing the hot well), a hot leg (circuit riser), a heat sink given by a heat exchanger bundle submerged in a pool, and a cold leg (circuit downcomer). Its operation is based on the high heat transfer capability of the steam generator, able to remove decay heat producing steam which is driven into riser piping. Steam condensation in a suitable heat exchanger permits to reject this heat to the environment via the pool. The circuit is closed by downcomer piping, which drains cold condensed water back to the steam generator.

Primary objective of this paper is to provide a deep analysis on the heat transfer phenomena involved in a component of the mentioned circuit, namely the condenser submerged in the pool. The two simplest and most used tube

configurations, which are horizontal tube and vertical tube arrangements, have been considered. Condensation under the typical working conditions of a passive safety system for decay heat removal represents hence the topic of the paper. A key point is to carry out an open literature review on the most updated and reliable models and correlations to deal with flow pattern identification and heat transfer coefficient prediction, both for horizontal tube and vertical tube applications. Most of the proposed correlations were validated in the recent past thanks to suitable experimental campaigns in properly scaled facilities. Therefore, a short review on the experimental facilities in the frame of the explored condensation models has been provided to fully accomplish the review purpose of the paper.

A simple Matlab code has been then developed in order to test and compare the various condensation models described in the paper, with the main purpose to quantify the better thermal-hydraulic performances offered by vertical tube arrangement for the in-pool condensers (fixed the proper reference conditions for the comparison with horizontal tube arrangement). As a second goal, the accuracy and the wide applicability range of the classical modelling approach based on film condensation theory for vertical tube applications have been corroborated thanks to experimental findings from PERSEO facility [2].

The present work is structured as follows: in Section 2 an overview on the various passive safety systems for decay heat removal implemented in GenIII+ nuclear reactors is presented; in Section 3 the review of condensation models (both for horizontal tube and vertical tube applications) is provided. The Section 4 is dedicated to the short review of the experimental facilities of main interest for condensation modelling issues. In the Section 5 the results obtained with the simple in-house code are discussed; finally in the Section 6 the validation of the proposed vertical tube condensation model based on film condensation theory is provided by means of PERSEO experimental data.

2. Review of Passive Safety Systems for Decay Heat Removal

A first concept of in-pool immersed heat exchangers deals with a parallel arrangement of horizontal U-tubes between two common headers. This configuration has been provided in the emergency condenser of a SWR1000 [3], as shown in Figure 1. The top header is connected via piping to the reactor pressure vessel steam plenum, while the lower header is connected to the reactor vessel below the water level. The heat exchangers are located in a lateral pool filled with cold water, forming a system of communicating pipes with the vessel. At normal reactor water level the emergency condensers are flooded with cold water; if a reactor trip occurs the level can drop so that the heat exchanging surfaces inside the tubes are gradually uncovered. The incoming steam condenses on the cold surfaces, and the condensate is simply returned to the reactor vessel, avoiding any core uncovering.

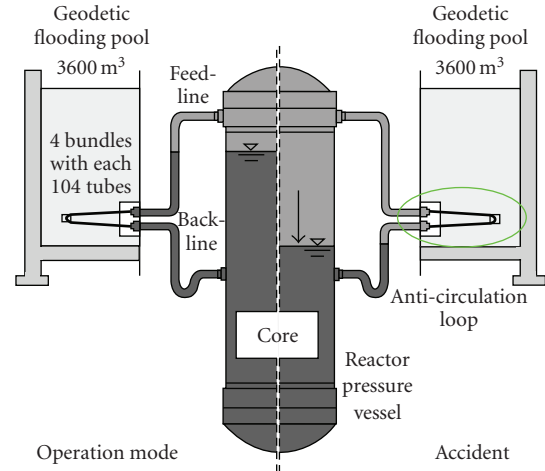


FIGURE 1: Emergency condenser of the SWR1000.

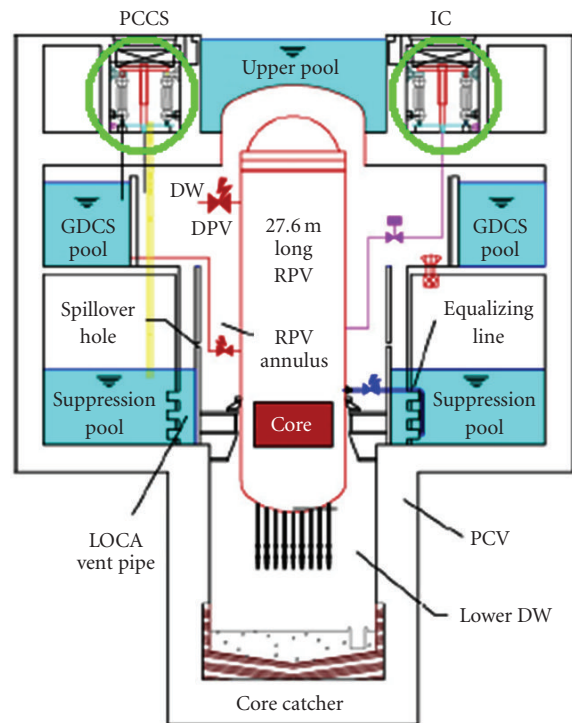


FIGURE 2: Isolation Condenser (IC) of the SBWR.

Other advanced water reactors implemented a vertical tube arrangement. This configuration has been carried out, for example, in the Isolation Condenser (IC) of an SBWR and in the Passive Containment Cooling System (PCCS) of a KNGR. In both cases decay heat is removed passively from the containment by the condenser submerged in a suitable pool [4].

In an SBWR [5] the system ICs are designed to passively limit the reactor pressure under accident conditions, whereas the containment ICs have to remove the decay heat after a LOCA. The physical location of the ICs is above the RPV, Suppression Pools and Gravity Driven Cooling System

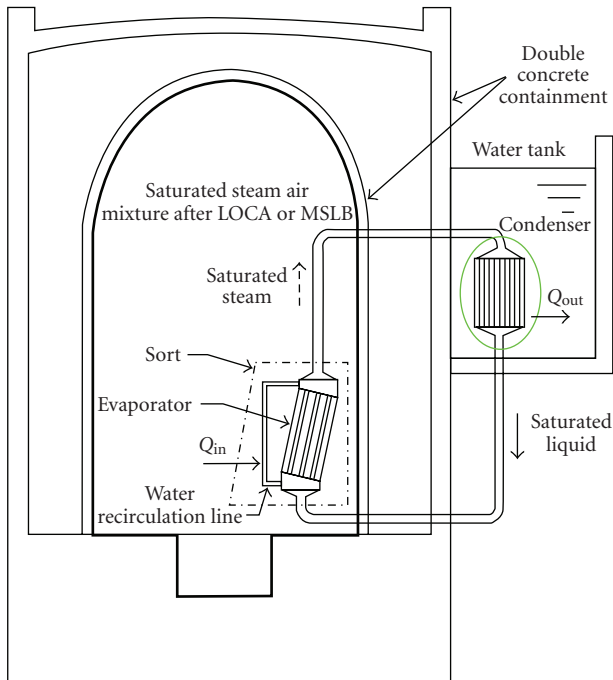


FIGURE 3: PCCS condenser of the KNGR.

(GDCS) in order to utilize the gravity induced return flow of the condensate from the ICs to the respective ports. Reactor layout is reported in Figure 2. Steam flows into the system ICs directly from the RPV, while the ICs of the PCCS receive a pressurized steam-nitrogen mixture from the drywell of the containment. Condensate is returned to the vessel by drain lines or through GDCS.

The PCCS of a KNGR [6] (Figure 3) is rather similar to the passive containment cooling system described for the SBWR ICs. It is provided with two heat exchangers, relevant lines and water tanks, and guarantees a way of external containment cooling through a natural circulation circuit. Heat transferred from the containment atmosphere to the coolant through the primary heat exchanger tubes is simply removed by condenser tubes to the water tank, located outside the containment.

A suitable passive safety system for decay heat removal, namely the Emergency Heat Removal System (EHRS) depicted in Figure 4, is foreseen also for IRIS reactor [7]. A previous in-pool condenser concept with horizontal U-tubes moved to a vertical tube arrangement; the utilization of the Isolation Condenser adopted from SBWR is now envisaged within the current design status. The Korean SMART reactor is conceived according to a similar idea of modular and integral-layout reactor; decay heat removal function is accomplished by the natural circulation in the PRHRS [8] (Figure 5), based again on steam generators for heat extraction and on in-pool heat exchangers (submerged in the Emergency Cooldown Tank -ECT-) for heat removal to the environment. A vertical tube arrangement is proposed.

The various decay heat removal systems developed for GenIII+ reactors point out a predominance of vertical

tube condensers, which offer on the whole better thermal-hydraulic performances, as it is shown in the followings. It is just mentioned that the heat transfer performance is not the only figure of merit to be accounted when choosing the most proper configuration for an in-pool condenser. Thermo-mechanical issues are indeed of critical importance: horizontal tube condensers, allowing inherently thermal expansions, are of course preferable rather than a straight single-pass vertical solution which could induce dangerous thermal stresses due to prevented dilatations. These issues lie anyway outside the interests of the paper, hence will not be covered in the analysis.

3. Literature Review of Condensation Models

The better heat transfer performances assured by a vertical pipe condenser, mainly in terms of higher heat transfer coefficient and more predictable in-tube flow distribution, are first briefly summarized. The typical conditions for the utilization of an in-tube condenser within one of the passive safety systems mentioned above have been taken as reference. The capability to remove about 20–30 MW of thermal power, inducing low mass fluxes $-G < 100 \text{ kg/sm}^2$ in the loop, is required.

Condensation in horizontal tubes is strongly influenced by the flow pattern, which can range from annular to stratified without avoiding the intermittent regimes (slug-plug). In a defined interval of mass fluxes and qualities, in fact, the possibility of fluid pulsation is concrete, driven by large amplitude waves that wash the top of the tube; flow reversal can be induced, as well as mechanical and thermal fatigue problems on the tube wall. A fully stratified-stratified wavy regime occurs according to the low flowrates and the medium-high pressures which characterize a natural circulation loop for DHR (typically 60–100 bar). A thin condensate film drains down from the upper part of the tube under the influence of gravity force, while a water sump accumulates and flows on the bottom. The HTC is negatively affected by this sump, in particular when it approaches subcooling conditions at the end of the pipe. Interfacial wave effects, increasing with the flowrate, do not balance this drawback. The result is an average heat transfer coefficient of approximately $4000\text{--}6000 \text{ W/m}^2\text{K}$ (considered a G equal to 60 kg/sm^2). Therefore, condensation in a horizontal tube deals with a whole of complex phenomena, which require a careful analysis.

Two-phase flow path is instead well defined in a vertical tube, in case of a downflow streaming. An annular film of condensate forms on the wall and falls down driven by gravity, filling up the cross-section only at the end and assuring a better condensation process along major portion of the pipe. Condensate flows with a higher velocity, reducing fouling and corrosion effects as well as assuring higher HTCs. At fixed quality, the higher velocities (pulled by gravity) lead to a thinner film, with a lower thermal resistance, a thinner laminar boundary layer and thus higher turbulence. Average heat transfer coefficients are strongly enhanced with respect to the horizontal solution, providing

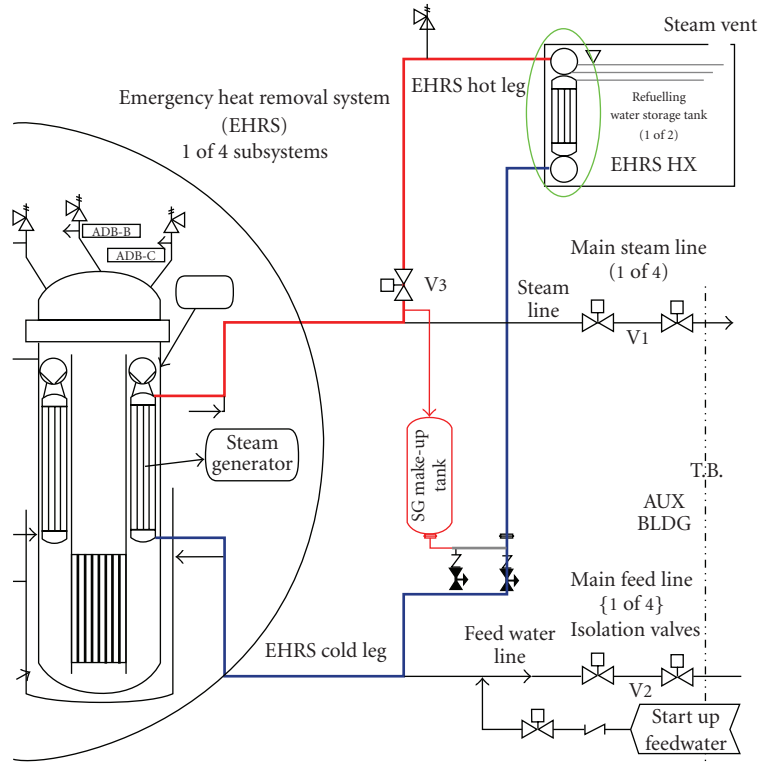


FIGURE 4: EHRH condenser of the IRIS.

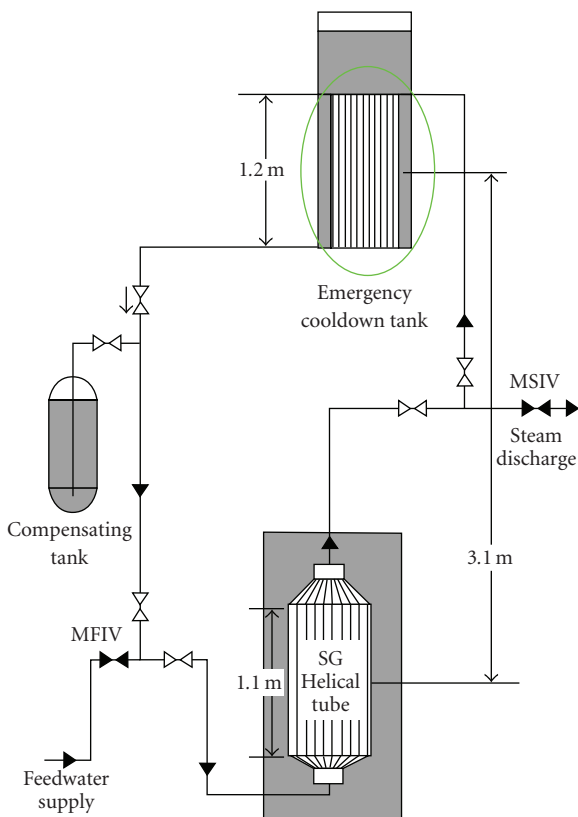


FIGURE 5: PRHRS condenser of the SMART.

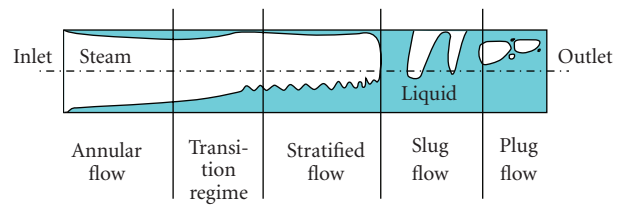


FIGURE 6: Different flow patterns during condensation in a horizontal tube.

values of approximately $8000\text{--}11000\text{ W/m}^2\text{K}$. A lack of high pressure steam condensation data for large diameter vertical tubes, which is indeed the case of the IC adopted from SBWR to IRIS, has been noticed in open literature works. A comprehensive investigation on how condensation is provided in a downflow vertical tube appears hence of great interest. The different physical phenomena involved within horizontal and vertical tubes are clearly shown by the drafts reported in Figures 6 and 7.

3.1. Modelling of Condensation in a Horizontal Tube. In early models [9–12], the flow patterns were classified just under two categories, that is, stratified or annular. The first, dominated by gravity forces, is characterized by a thick condensate layer flowing along the bottom of the tube, while a thin liquid film forms on the wall in the upper portion of

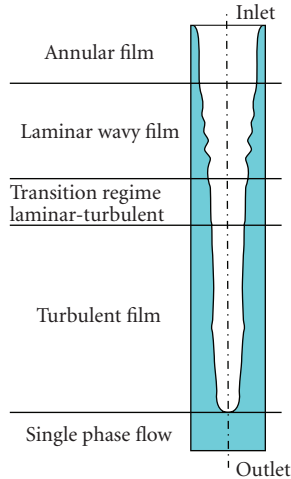


FIGURE 7: Different flow patterns during condensation in a vertical tube.

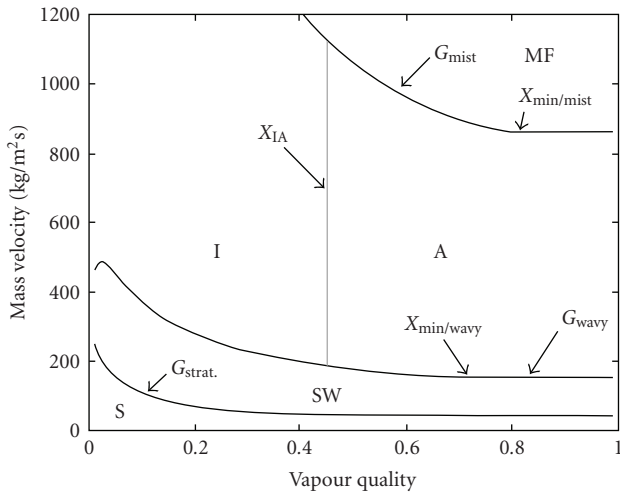


FIGURE 8: Thome's flow pattern map for condensation in a horizontal tube. S → stratified SW → stratified wavy A → annular I → intermittent MF → mist flow.

the tube. The latter, dominated by shear effects, leads to an annular ring of condensate flowing uniformly along the tube. Different flow regimes can be instead induced. When the stratified condensate layer in the tube sump reaches medium-high velocities, ripples or waves are often generated at the phase surface (stratified wavy). If these waves become so large to wash the top of the tube, an intermittent flow pattern (slug-plug) can be established, presenting a very complex flow structure. At very high velocities, finally, a mist (spray) regime can occur, characterized by impinging droplets on the thin unsteady liquid film.

Two models are proposed in this paper as the most updated and reliable concerning the condensation in a horizontal tube, each one based on a proper flow pattern map for the identification of the actual flow regime (reported, resp. in Figures 8 and 9).

In Thome's model [13–15] the intermittent (both slug and plug) and mist flows are considered and evaluated as

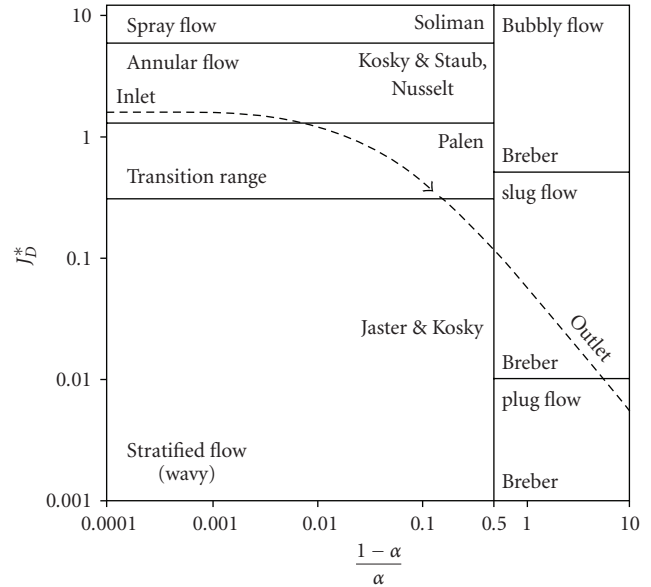


FIGURE 9: Tandon's flow pattern map for condensation in a horizontal tube.

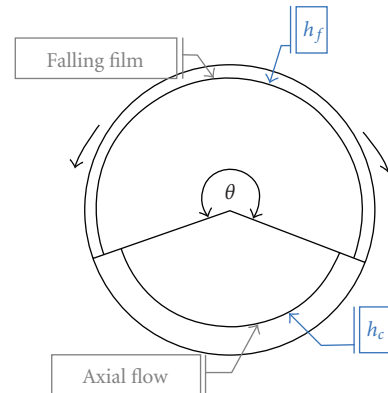


FIGURE 10: Heat transfer model showing convective and falling film.

annular flow. For annular flow a uniform film thickness is assumed and the actual larger thickness of the film at the bottom rather than the top due to gravity is ignored. Stratified and stratified wavy are instead characterized by the so named stratification angle, which subtends the cross-sectional area occupied by the liquid, assumed as truncated annular ring of uniform thickness. Figure 10 is useful to understand the provided simplifications. Two different heat transfer mechanisms are considered within the tube: convective condensation and film condensation. The first refers to the axial flow of condensate along the channel due to the imposed pressure gradient; the second refers to the flow of condensate from the top of the tube towards the bottom due to gravity. The convective condensation heat transfer coefficient h_c is applied to the perimeter wetted by the axial flow of liquid film, which is the entire perimeter in annular flow, but only part of the perimeter in stratified wavy and stratified one. The film condensation

heat transfer coefficient h_f , affecting only stratified–stratified wavy regime, is obtained by applying the Nusselt's falling film theory [16] to the inside of the horizontal tube, assumed a laminar falling film. Hence, the condensation HTC is given combining these two coefficients according to

$$h = \frac{h_f \theta D_i / 2 + h_c (2\pi - \theta) D_i / 2}{\pi D_i}. \quad (1)$$

The convective condensation heat transfer coefficient h_c can be obtained from the following film equation, assumed the axial flow as turbulent

$$h_c = 0.003 \text{Re}_i^{0.74} \text{Pr}_i^{0.5} \frac{k_l}{\delta} f_i \quad (2)$$

where δ is the film thickness, considered uniform in all the cross-section. This is an only liquid correlation type, that is, just the liquid part of the two-phase flowrate has to be considered, resulting

$$\text{Re}_i = \frac{4G(1-x)\delta}{(1-\alpha)\mu_l}. \quad (3)$$

The interfacial roughness correction factor f_i takes into account the shear effects which dominate an annular flow regime. First of all, the shear of the high speed vapour is transmitted to the liquid film across the interface. Magnitude and number of the interfacial waves are increased and hence available surface area for condensation, inducing an enhancement in heat transfer. Secondly, these interfacial waves tend to reduce the mean thickness of the film (and thus its thermal resistance), again increasing heat transfer. Interfacial roughness and wave formation are also directly relatable to entrainment of liquid droplets into vapour phase, which reduces the thickness of the liquid film and increases heat transfer. Finally, interfacial shear creates vortices within the liquid film, which also increase heat transfer.

The film condensation heat transfer coefficient h_f , instead, is given from a modification of the Nusselt's theory for laminar flow of a falling film outside a horizontal tube (around the perimeter, from top to bottom) applied indeed to the condensation on the inside. Any effect of axial shear on the falling film is ignored. According to theory, heat transfer coefficients are known to be a function of tube wall temperature difference (not noticeable nevertheless for annular flow). Typical heat exchanger design codes are being implemented taking as variable the heat flux in each incremental zone along the exchanger (rather than wall temperature difference); therefore the heat flux version of Nusselt's equation is better to be considered:

$$h_f = 0.655 \left[\frac{\rho_l (\rho_l - \rho_g) g \Delta h_{fg} k_l^3}{\mu_l D_i \Phi_i} \right]^{1/3}, \quad (4)$$

where Φ_i is the heat flux related to the internal diameter.

The heat transfer coefficient given by (4) has to be intended as average HTC when referred to tube average heat flux, whereas represents a local value when the tube length is divided into different nodes and local heat flux for each

node is accounted. In the same way, (2) gives a local HTC when the mean quality at half cell is considered in (3). All the computational details to calculate h_c and h_f can be anyway found in [13–15].

Schaffrath's model [17] was developed for the investigation of the operation mode of the SWR1000 emergency condenser (NOKO test facility). It is based on Tandon's flow regime map [18] for the determination of the actual flow regime and switches to flow regime semi-empirical correlations for the HTC calculation: Soliman for spray flow [19], Nusselt for laminar annular flow, Kosky and Staub for turbulent annular flow [20], Rufer and Kezios for stratified flow [21], Breber et al. for slug-plug flow [22]. The parameters chosen to identify the flow pattern are the dimensionless vapour velocity j_D^* and the volume ratio of liquid and gas in a cross-sectional area $(1-\alpha)/\alpha$.

3.2. Modelling of Condensation in a Vertical Tube. In a down-flow vertical pipe condensation takes place with a condensate film growing up in contact with the wall, while vapour phase flows along the bulk of the channel. Many methods have been proposed for predicting the film condensation heat transfer coefficient; these range from empirical or semi-empirical correlations to highly sophisticated analytical treatments of the transport phenomena [23–25].

In this work the classical modelling approach, based on Nusselt's analysis [26] for film condensation on a vertical plate, is adapted to the inside of a vertical tube. Mass, momentum and energy equations for the condensate film are dealt according to the following assumptions [16]:

- (i) Pure vapour and at saturation temperature is considered. With no temperature gradient in the steam, heat transfer can occur only by condensation at the interface.
- (ii) Shear stress at the liquid-vapour interface is neglected.
- (iii) Advection terms in the equations are assumed to be negligible. Heat transfer across the film occurs only by conduction. Liquid temperature distribution is thus linear, and this concern can be expressed as

$$Nu_l = \frac{h\delta}{k_l} = 1. \quad (5)$$

The distinction of film condensation into three different regimes has been provided, according to the different physical phenomena which can occur: laminar, laminar wavy and turbulent. Figure 11 is useful to understand the flow patterns induced inside the tube.

The analytical solution of the governing equations, passing through the calculation of condensate film thickness δ , allows treating laminar regime. Semi-empirical correlations are recommended for laminar wavy and turbulent regimes. The main parameter governing the process is the condensate velocity, expressed by its Reynolds number Re_l as follows:

$$\text{Re}_l = \frac{4\Gamma_l}{\pi D_i \mu_l}, \quad (6)$$

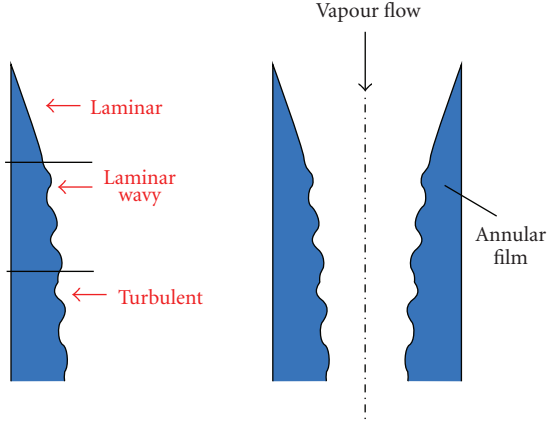


FIGURE 11: Sketch of film condensation inside a vertical tube.

where Γ_l is the liquid flowrate, to be expressed according to an only liquid approach:

$$\Gamma_l = \Gamma(1 - x). \quad (7)$$

(i) *Laminar* $Re_l < 30$. Condensation HTC's decrease in the laminar region with increasing film thickness due to the increased thermal resistance. Nevertheless, laminar condensation occupies a very short portion of the tube and hence can be neglected in the calculations:

$$h = k_l \left(\frac{\gamma_l^2}{g} \right)^{-1/3} 1.1 Re_l^{-1/3} \quad \text{Nusselt correlation.} \quad (8)$$

(ii) *Laminar wavy* $30 < Re_l < Re_{tr} = 4658 Pr_l^{-1.05}$. Condensation HTC's (still a decreasing function of film thickness) are enhanced when the film becomes wavy, because waves promote turbulence in the film and increase heat exchange surface [27]. Re_{tr} represents the transition value between laminar (wavy) and turbulent film condensation:

$$h = k_l \left(\frac{\gamma_l^2}{g} \right)^{-1/3} 0.756 Re_l^{-0.22} \quad \text{Kutateladze correlation.} \quad (9)$$

(iii) *Turbulent* $Re_l > Re_{tr} = 4658 Pr_l^{-1.05}$. The highest HTC's are provided once the film has become turbulent; the trend is now different from previous case (being the HTC an increasing function of film thickness), due to mixing effects which exceed the higher thermal resistance. Two different semi-empirical correlations can be applied [28, 29]:

$$h = k_l \left(\frac{\gamma_l^2}{g} \right)^{-1/3} 0.023 Re_l^{0.25} Pr_l^{0.5} \quad \text{Labuntsov correlation,} \quad (10)$$

$$h = k_l \left(\frac{\gamma_l^2}{g} \right)^{-1/3} 0.00402 Re_l^{0.4} Pr_l^{0.65} \quad \text{Chen correlation.} \quad (11)$$

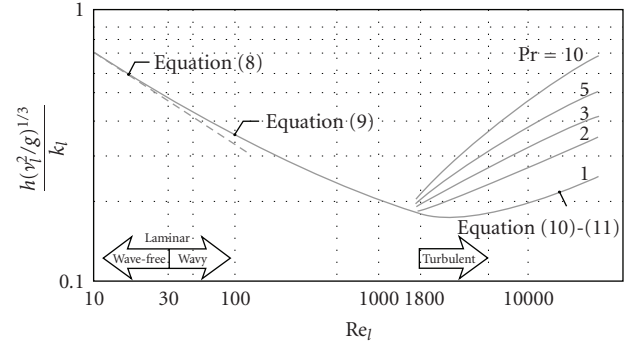


FIGURE 12: Nondimensional HTC dependence on condensate Reynolds number, for condensation on a vertical plate [16].

Figure 12 shows nondimensional heat transfer coefficient dependence on condensate Reynolds number Re_l , which increases in the downward direction inside the tube [16]. Above discussed HTC trends find their confirmation.

All the proposed correlations give a local HTC value. A general expression providing an average heat transfer coefficient is more useful especially in design applications. The easiest way to calculate average heat transfer coefficients is to integrate the equations for local coefficients along the tube length, resulting:

$$\bar{h}_L = \frac{1}{L} \int_0^L h(s) ds. \quad (12)$$

The following correlations can be considered in order to compute the mean HTC for the various flow regimes:

(i) *Nusselt* correlation for laminar zone, obtained analytically integrating (8) from $s = 0$ to $s = L$ [16]:

$$\bar{h}_{lam} = k_l \left(\frac{\gamma_l^2}{g} \right)^{-1/3} 1.47 Re_L^{-1/3}. \quad (13)$$

(ii) *Kutateladze* correlation for laminar wavy zone [27]:

$$\bar{h}_{lam-wavy} = k_l \left(\frac{\gamma_l^2}{g} \right)^{-1/3} \frac{Re_L}{1.08 Re_L^{1.22} - 5.2}. \quad (14)$$

(iii) *Labuntsov* correlation for turbulent zone [28]:

$$\bar{h}_{turb} = k_l \left(\frac{\gamma_l^2}{g} \right)^{-1/3} \frac{Re_L}{8750 + 58 Pr_l^{-0.5} (Re_L^{0.75} - 253)}. \quad (15)$$

(iv) *Blangetti* correlation for turbulent zone [30]:

$$\bar{h}_{turb} = k_l \left(\frac{\gamma_l^2}{g} \right)^{-1/3} \frac{Re_L}{414.6 Re_L^{0.6} Pr_l^{-0.65} - 5.182 - 33514 Pr_l^{-1.27}}. \quad (16)$$

(v) *Chen* correlation for the total film condensation (neglecting laminar and considering both laminar wavy and turbulent zones) [29]:

$$\bar{h} = k_l \left(\frac{\gamma_l^2}{g} \right)^{-1/3} (Re_L^{-0.44} + 5.82 \cdot 10^{-6} Re_L^{0.8} Pr_l^{1/3})^{1/2}. \quad (17)$$

Usually the Shah correlation [31], which is an empirical correlation based on a wide range of experimental data, is mostly considered as the best correlation for the turbulent film condensation heat transfer both in horizontal, vertical and inclined pipes. It is based on a liquid only approach, referring the two-phase HTC to the single-phase coefficient computed with Dittus-Boelter correlation, assumed all the flowrate being liquid:

$$h = h_l \left[(1 - x)^{0.8} + \frac{3.8x^{0.76}(1 - x)^{0.04}}{p_r^{0.38}} \right] \quad \text{local HTC, (18)}$$

$$\bar{h} = h_l (0.55 + 2.09 p_r^{-0.38}) \quad \text{mean HTC. (19)}$$

Nevertheless the validity of Shah correlation is questionable for high pressure and large diameter tube applications with water, as recently experimentally confirmed by Kim and No [32]. Moreover, this correlation predicts a decreasing HTC with a decreasing quality, exactly the opposite trend of film condensation theory. It is also questionable how the same correlation could be suitable for all the flow orientations, since the physical phenomena involved are rather different.

4. Short Review on Experimental Facilities

In the frame of advanced water reactors development, the construction of experimental facilities is required to study the behaviour of integral systems during postulated accidents as well as separate effect phenomena on specific innovative components. This section is dedicated to the brief discussion of the experimental works carried out to fully qualify in-pool condenser systems and validate the proper modelling tools for condensation analyses.

Suitable facilities, built and operated in the recent years, provided a large amount of data, based on which the heat transfer correlations (both for horizontal and vertical tube configurations) were validated. Best-estimate thermal-hydraulic code assessment on such data is then the final task in order to guarantee the availability of reliable computational tools to duly perform special components design and reactor safety analyses.

The NOKO test facility was constructed at the Forschungszentrum Jülich for the experimental investigation of the SWR1000 emergency condenser effectiveness [3]. The design of the facility, provided with an operating pressure of 10 MPa and an electrical heater with a maximum power of 4 MW, permits to adjust the same thermal-hydraulic conditions as in the real plant; moreover, prototypical elevations, water levels, dimensions and HX tubes material have been reproduced. A phenomenological evaluation was performed to determine the operation conditions of the emergency condenser. The HX capacity was determined as a function of primary pressure, pool pressure and water level, as well as of concentration of the non-condensables in the vessel. The experimental results showed that extracted thermal power increases with a primary side pressure increase and decreases with a pool side pressure increase. The emergency condenser characterization was accomplished

calculating the tube surface available for condensation by means of the evaluation of geodetic pressure drops variation in consequence of vessel water level decrease. A single tube test, besides, was provided to clarify the condensation flow regimes inside a horizontal tube and to validate Tandon's flow map condensation model (reported in Figure 9). This experimental campaign led finally to the improvement of ATHLET thermal-hydraulic code [17], implementing the correlations discussed at the end of Section 3.1.

The long-term decay heat removal from the containment of advanced light water reactors, and in particular the long-term LOCA response of the Passive Containment Cooling System of the ESBWR, were tested in the large scale PANDA facility [33]. Constructed at the Paul Scherrer Institute (PSI) for the investigation of both overall dynamic response and key phenomena of passive containment systems, it consists briefly of six vertical cylindrical vessels, four water pools and a variety of connecting lines available to compose different facility configurations. The major aspect of the tests dealt with the evaluation of the ESBWR PCCS performance in case of main steam line break. Released steam flows into the drywell where it is mixed to the air contained inside; then the mixture is vented into the wetwell where the steam content is condensed and the air content is separated, inducing an increase in system pressure. When the heat exchangers in the pool start their operation, condensation of the steam-air mixture allows stopping pressure increase. Pressure time behaviour defines thus the response of the whole system to the specific transient. As far as condensation issues are concerned, PANDA facility was very useful for investigating the degradation of HTC (and then the influence on the effective condensing length) in presence of non-condensable gases [34], both heavier than steam, initially filling the containment compartments (nitrogen or air), and lighter than steam, released later in the course of the transient from the reactor core (hydrogen, simulated by helium). The provided tests permitted moreover to extend the database available for containment analysis code qualification.

The VISTA facility is the experimental facility developed by the KAERI to simulate the primary and secondary systems as well as the PRHRS of the SMART reactor [8]. The main objective of the study was to investigate the characteristics of natural circulation flows, passive system pressure drops and heat transfer performances of the PRHRS heat exchangers. The secondary objective was to confirm the capability of MARS best-estimate code to predict the overall thermal-hydraulic behaviour of the PRHRS. One of the most important results was that the code underestimated heat transfer at the heat exchanger, predicting fluid temperatures at HX bottom higher than the experimental results. The condensation model used in the code, exactly the same of that adopted by RELAP5 code [35], considers the maximum value between Nusselt correlation (8) for laminar flow and Shah correlation (18) for turbulent flow. The implementation in MARS and RELAP5 codes of suitable heat transfer correlations, as the ones proposed in this paper on the bases of film condensation theory, would guarantee a more accurate heat transfer package to duly carry out transient and safety analyses.

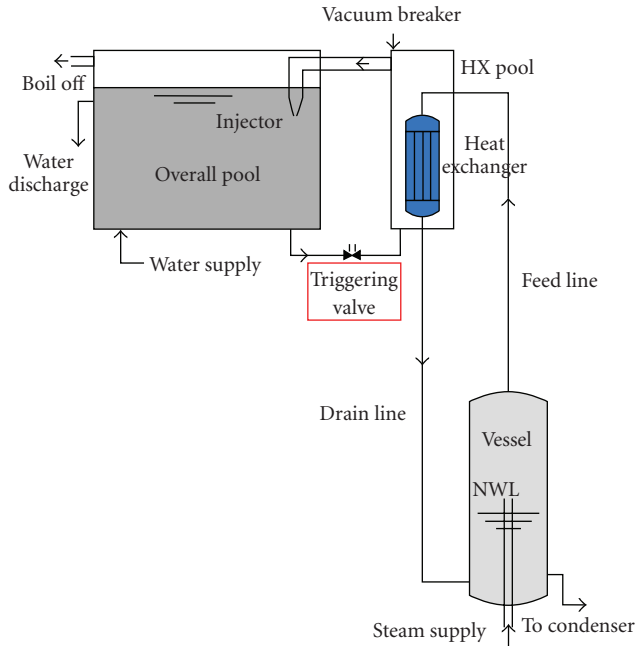


FIGURE 13: PERSEO facility scheme.

In spite of the common belief that passive systems should not require any operator actions, the actuation of such systems needs to be started by active valves, whose reliability is of fundamental importance. A new concept of a valve liquid side, instead of steam side in the primary system, located on a line connecting two pools at the bottom, has been proposed in the PERSEO facility [2] (Figure 13), developed in SIET labs (Piacenza) for testing a full scaled module for the GE-SBWR in-pool heat exchanger. The full scale module of the SBWR IC consists in two horizontal cylindrical headers and 120 vertical pipes; prototypical thermal-hydraulic conditions were respected, reproducing the removal to the pool of heat exchanger nominal power ($20 \text{ MW}_{\text{th}}$) by means of the supply of saturated steam at 7 MPa from the nearby EDIPOWER power station. The new kind of actuation valve (named triggering valve) is closed during normal operations and the pool containing the heat exchanger (HX pool) is empty; the other pool (Overall pool) is full of cold water. Under emergency conditions the valve is opened and the heat exchanger is flooded, with consequent heat transfer from the primary side to the pool. The effectiveness of the actuation valve movement, from the high pressure primary side of the reactor to the low pressure pool side, was tested during the experimental campaign, both in steady and in unsteady conditions. Two kinds of tests were performed: integral tests and stability tests. The integral tests were aimed at demonstrating the behaviour and performance of the system following a request of operation and during all phases of a long accident transient. The stability tests, instead, were aimed at studying particular critical problems happening in case of sudden condensation at the steam water interface in the injector or in case of triggering valve re-opening, with cold water inlet in presence

TABLE 1: IC data, taken as reference for the calculations.

Parameter	Choice
Tube outer diameter	50.8 mm
Tube inner diameter	46.2 mm
Tube thickness	2.3 mm
Thermal conductivity	17.4 W/mK
Pressure	72.4 bar
Fouling	$5 \cdot 10^{-5} \text{ m}^2\text{K/W}$
Plugging	5% of tubes
Thermal power	35 MW
Number of tubes	240 (2 units of IC)
Flowrate per tube	0.103 kg/s
Mass flux G	61.47 kg/sm ²

of steam in the HX pool. The experimental testing of the IC in-pool condenser concept provided moreover a useful database for condensation models validation. Within the postprocessing analysis on PERSEO project results [36], the finding of experimental data for condensation inside a vertical tube has been envisaged in order to validate the heat transfer correlations proposed in this paper.

5. Calculation Results

Proposed condensation heat transfer models, both for application within horizontal and vertical tubes, have been firstly verified through the development of a simple Matlab code. The reference case was taken from set of PERSEO test data, being the primary aim to show with simple calculations (without the utilization of a best-estimate code) how a vertical tube configuration can guarantee the highest HTC_s in condensation, as well as the best trend (i.e., increasing along tube abscissa). The step-by-step computational procedure followed in the calculations, in order to obtain condensation HTC trend along tube abscissa and the actual length required to accomplish design prescriptions, is described in the appendix.

Table 1 summarizes the data of SBWR IC mean tube design representing the basis for the analysis. The reference tube is thus a vertical tube, with an inner diameter of 46.2 mm and an outer diameter of 50.8 mm, submerged in a pool of boiling water at 100°C. Tube material is INCONEL 600 (17.4 W/mK of thermal conductivity), and fluid inlet conditions are represented by saturated steam at 72.4 bar. The utilization of this HX within the EHRS of IRIS reactor has been taken into account. Hence, following design prescriptions, two units of the condenser (with 120 tubes each one) have to exchange altogether a thermal power of 35 MW. Fouling effects, both for internal and external side, are quantified with an additional thermal resistance of $5 \cdot 10^{-5} \text{ m}^2\text{K/W}$, while a possible plugging of the 5% of the tubes is also considered. The resulting reference value of flowrate per tube is equal to 0.103 kg/s, which gives a mass flux G equal to 61.47 kg/sm².

Reference data for the calculations are related to a condenser with vertical tube arrangement. Nevertheless, they

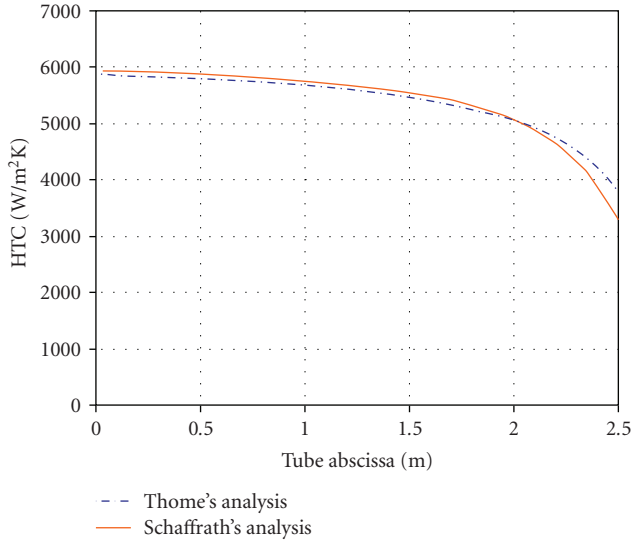


FIGURE 14: Comparison between Thome's analysis and Schaffrath's analysis in stratified flow ($G = 61.5 \text{ kg/sm}^2$).

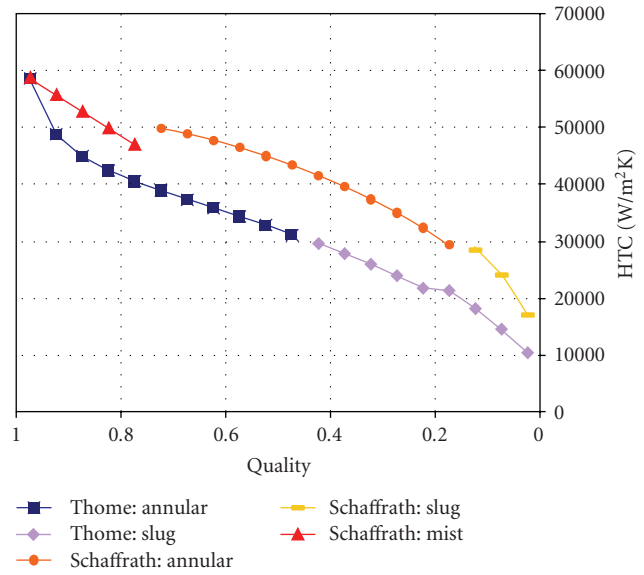


FIGURE 16: Comparison between Thome's analysis and Schaffrath's analysis at very high flowrates ($G = 984.8 \text{ kg/sm}^2$).

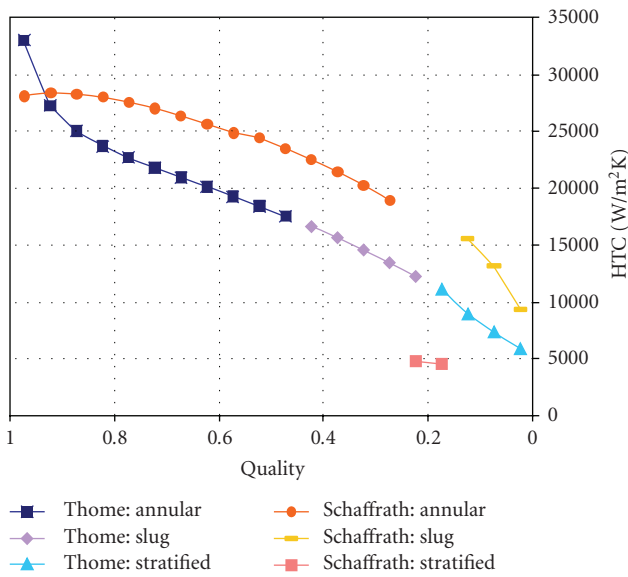


FIGURE 15: Comparison between Thome's analysis and Schaffrath's analysis with dominant annular flow ($G = 417.6 \text{ kg/sm}^2$).

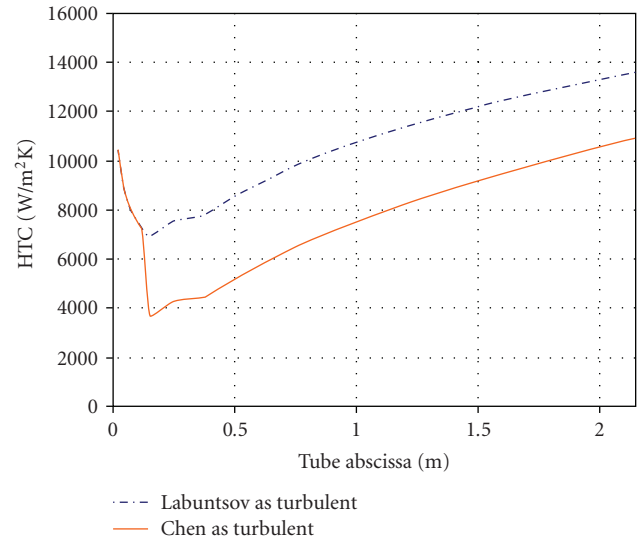


FIGURE 17: Condensation HTC along tube abscissa, according to film condensation theory ($G = 61.5 \text{ kg/sm}^2$).

have been applied also to test the models for horizontal in-tube condensation and provide thus a proper comparison with the vertical tube arrangement results. In case of condensation within a horizontal tube, reference value of mass flux leads to a stratified pattern. Heat transfer coefficient trend along the pipe has been predicted, applying first Thome's analysis and then Schaffrath's model, selected the proper correlation (Rufer and Kezios formula). The tube length required to completely condense the inlet steam (with saturated liquid at condenser outlet) is evaluated as 2.50 m. A pretty fair agreement can be observed between the two distinct models, as shown in Figure 14: an average heat transfer coefficient of approximately $5500 \text{ W/m}^2\text{K}$ involves

almost the entire length, decreasing just at the end. When condensate starts to occupy the major portion of cross-sectional area, in fact, the condensate sump dominates any type of film condensation at the top of the tube. The higher thermal resistance causes the lower heat transfer coefficient. Moreover, the possibility of a slug-plug flow (at low qualities, with $x < 0.1$) is envisaged by Schaffrath's analysis. Condensation in a horizontal tube proves thus to be a complex phenomenon, considered the risk of instabilities which could derive from the intermittent flow regimes.

Thome's and Schaffrath's models have been tested even under high flowrate conditions, establishing flow regimes different from stratified pattern. Two distinct values of

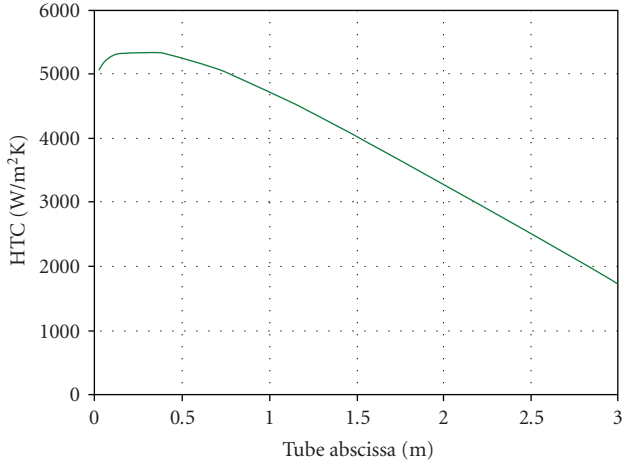


FIGURE 18: Condensation HTC along tube abscissa, according to Shah correlation ($G = 61.5 \text{ kg/sm}^2$).

inlet flowrate have been considered: 0.7 kg/s , which gives a dominant annular flow, and 1.5 kg/s , which induces a mist flow at tube entrance. Respective results are reported in Figures 15 and 16. It is evident that heat transfer coefficient increases with flowrate (for turbulence development). Such trend is confirmed in similar ways by the two models. Tandon's map provides for annular flow ($\Gamma = 0.7 \text{ kg/s}$) a HTC value slightly higher and less variable along the tube. Thome's analysis, finally, is not capable of treating separately the spray flow; nevertheless, the results obtained when dealing with annular flow at $\Gamma = 1.5 \text{ kg/s}$ are rather similar to HTC values given by Soliman correlation, the one selected in Tandon's map for the mist regime.

The same calculational model has been then applied implementing the vertical tube correlations. Predicted tube length is equal to 2.17 m according to film condensation correlations, and to 3.04 m for Shah correlation. The first model is certainly more accurate, being based on physical principles; hence, it is evident that for the IC conditions of pressure, flowrate and tube diameter (globally representative of the typical working conditions for an in-pool immersed HX within DHR applications), Shah's model broadly underpredicts the condensation HTC. Moreover, an opposite trend of turbulent heat transfer coefficient with a quality decrease is confirmed between the two models (increasing for film condensation, but decreasing for Shah's model). The comparison is provided by the graphs reported in Figures 17 and 18. As far as film condensation is concerned, laminar zone is absolutely negligible, and laminar wavy zone (with its decreasing trend of HTC with tube abscissa) is noticed up to a quality value of 0.95 . As regards turbulent zone, both Labuntsov and Chen correlations have been implemented. The latter gives lower HTCs, proving to be more conservative (and hence it has been used in sizing calculations). Chen correlation for mean HTC along the tube predicts a value of approximately $8000 \text{ W/m}^2\text{K}$. When comparing these outcomes (except for the ones obtained with Shah correlation, whose validity is however highly questionable) with the

predictions of horizontal tube models, it is evident that the vertical tube is in position to assure better performances, first just resulting in higher heat transfer coefficients. A direct consequence of this concern is the increased length required by horizontal tubes to completely condense the inlet steam (i.e., 2.50 m compared to 2.17 m of the vertical configuration). At the end, it is noted that Shah correlation prescriptions limit its validity to 40 mm of inner diameter, below the inner diameter of the IC tube under examination. The extrapolation of Shah correlation outside the range of the covered parameters appears a sufficient explanation for the wrong HTCs predicted.

6. Experimental Findings from Perseo Facility

Experimental findings useful for validating the vertical tube condensation model proposed in this paper represent one important result of PERSEO facility campaign. Thanks to the collaboration between POLIMI and SIET, such experimental findings have been analyzed, focusing the interest on condenser inner side performance. Main results are discussed in this section.

Some IC tubes were monitored with wall thermocouples (K-type, nominal accuracy of $\pm 1.5^\circ\text{C}$), applied on the outer surface at three different axial positions: at the top, at the middle and at the bottom of tubes. Circuit pressure (equal to 7 MPa) was measured with a pressure transmitter installed inside HX upper header, whereas primary flowrate (on average 0.1 kg/s per tube) was measured by an orifice differential pressure transmitter (with an uncertainty of $\pm 0.25\%$ of the instrument full scale). Due to the lack of accuracy of fluid thermocouples, saturated steam has been considered at condenser inlet and saturated liquid at condenser outlet. This assumption permitted to calculate the exchanged thermal power, and then to obtain the local heat flux required for heat transfer coefficients computation. Saturation temperature at the circuit pressure has been adopted as fluid bulk temperature, while inner wall temperature has been calculated from tube external value (measured) adding the thermal jump in the metal, resulting

$$T_{w,i} = T_{w,e} + \frac{D_i \ln(D_e/D_i)}{2k_{\text{tube}}} \Phi_i. \quad (20)$$

For each thermocouple position the local heat flux value Φ and the local HTC h_{cond} have been obtained by solving the following system of two equations, where $T_{w,i}$ must be calculated according to (20):

$$\begin{aligned} U_i &= \frac{\Phi}{T_{\text{sat},i} - T_{\text{sat},e}} \\ &= \left(\frac{1}{h_{\text{cond}}} + \frac{D_i \ln(D_e/D_i)}{2k_{\text{tube}}} + \frac{1}{h_{\text{pool}}(D_e/D_i)} \right)^{-1}, \quad (21) \\ h_{\text{cond}} &= \frac{\Phi}{T_{\text{sat},i} - T_{w,i}}. \end{aligned}$$

The sketch of the accounted situation is depicted in Figure 19. The obtained results are presented in Figure 20,

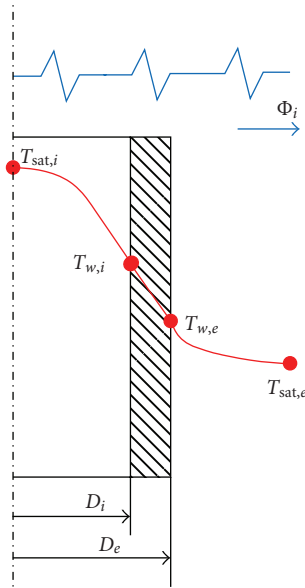


FIGURE 19: Sketch of heat transfer and temperature distribution in a single tube.

where they are compared to the predictions of film condensation theory (in particular, Kutateladze correlation for laminar wavy zone and Chen correlation for turbulent zone) and of a semi-empirical model proposed by Kim and No [32]. The increasing HTC trend and the good accordance with the experimental values confirm the validity of the proposed correlations, confuting therefore the Shah correlation under these particular thermal-hydraulic conditions (i.e. condensation of water steam at high pressure in large diameter vertical tubes). Among the works available in literature questioning about the validity of Shah's model, the experimental work of Kim and No has been selected since the investigated test section consists in a tube with the same geometrical features of the SBWR IC tested in PERSEO facility (i.e., outer diameter of 50.8 mm, thickness of 2.3 mm and length of 1.8 m). The semi-empirical model validated on Kim's data is a turbulent film condensation model based on the similarity between the single-phase turbulent convective heat transfer and the annular film condensation heat transfer. For any computational detail, refer to [32].

Figure 20 shows a remarkable shifting between theory and experimental data only at the end of the tube, where the liquid film at the wall cannot be considered any more as thin. This is proved by the void fraction damping down at the bottom of the pipe, which questions the validity of the presented theory. Figure 21 presents the comparison of PERSEO data with Kim's data; both Kim's model and Shah correlation (18) have been considered in order to predict the experimental values. HTCs calculated from PERSEO data are rather higher than HTCs calculated from Kim's data; the higher condensate Reynolds numbers reached in PERSEO facility are a plausible explanation of this concern. The order of magnitude is however well captured. Moreover, both the databases confirm that Shah's model is not accurate when

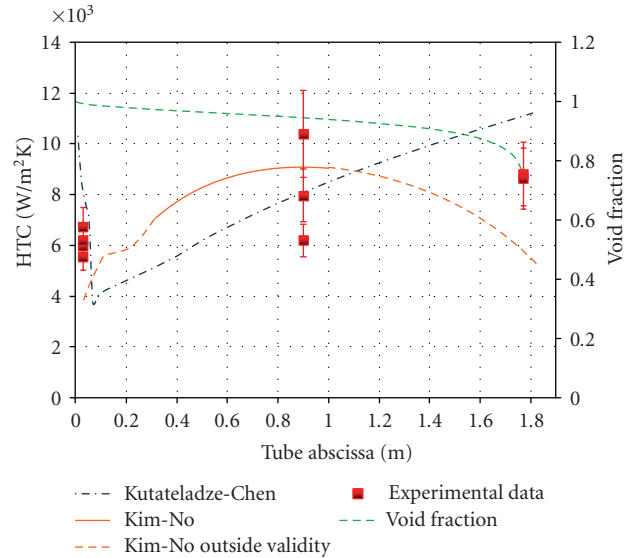


FIGURE 20: PERSEO facility experimental data compared with film condensation theory and Kim's model [32] predictions.

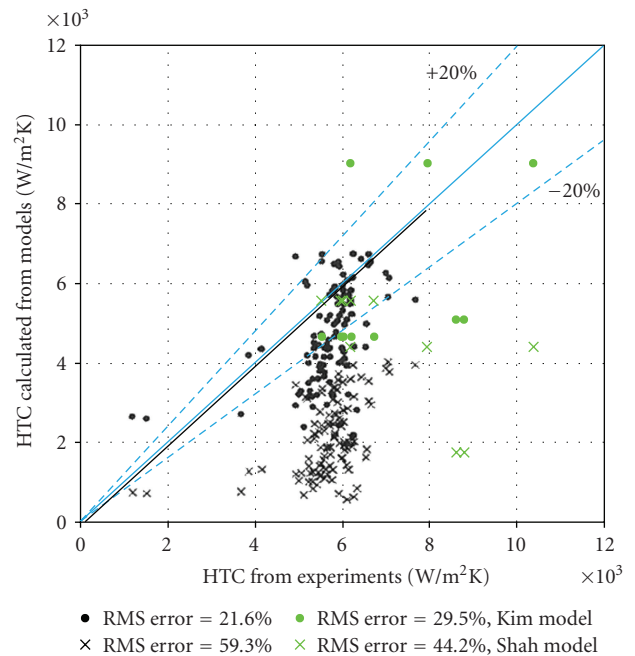


FIGURE 21: Comparison between PERSEO facility data (green) and Kim's data (black).

dealing with condensation phenomena at high pressure, whereas the semi-empirical model validated on Kim's data gives more satisfactory results.

At the end, the film condensation model based on Kutateladze correlation (9) and Chen correlation (11) has been considered to predict PERSEO data. The results, distinguishing between the predictions at the top, at the middle and at the bottom of tubes, are reported in Figure 22. The set of correlations proposed in this paper offers the best agreement with PERSEO data, whereas the turbulent annular

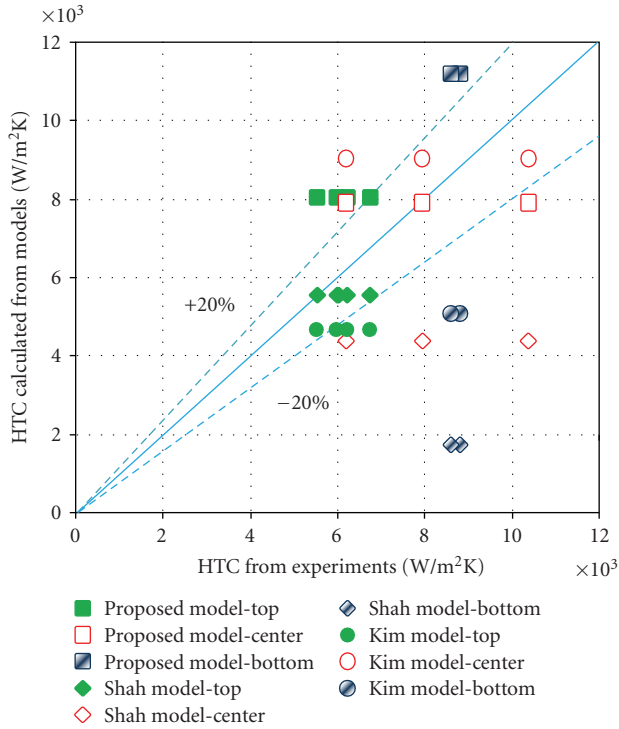


FIGURE 22: Benchmark evaluation of PERSEO data according to the various condensation models.

condensation model proposed by Kim fails at low qualities (when condensate Reynolds number becomes too high at the end of the tube). Except for tube inlet (high qualities), Shah’s model broadly underestimates the condensation HTC.

7. Conclusions

In the frame of the study on innovative passive safety systems and components, which require the proper modelling tools for the analysis of the heat transfer phenomena involved, an accurate review on the concept of in-pool condenser for DHR applications has been the main purpose of the work. Primary objective has been to provide a literature review of the most updated and reliable heat transfer models for condensation both in horizontal and in vertical tube condensers, which are the two most used configurations. The conditions at which condensation has been considered in the paper are such that are typical of passive safety systems for decay heat removal.

An overview on the concept of in-pool condenser within a DHR passive safety system has been firstly carried out. A preponderance of vertical tube arrangement solution has been pointed out for applications to GenIII+ nuclear reactors. The main advantages offered by a downflow vertical configuration are

- (i) higher heat transfer coefficients (even doubled with respect to horizontal solution),
- (ii) more predictable in-tube flow distribution.

Two calculational models have been presented as far as horizontal in-tube condensation is concerned. The first model is based on Thome’s work, distinguishes between three different flow regimes (annular, stratified and stratified wavy) and takes into account two heat transfer mechanisms: convective condensation and film condensation. The second model is based on Tandon’s map, as proposed by Schaffrath. Condensation within a vertical tube has been addressed according to a physical principle analysis, relied on film condensation theory for a vertical plate. In this paper the classical modelling approach based on the Nusselt’s theory for laminar film condensation has been presented. Suitable semi-empirical correlations have been proposed for laminar wavy regime (Kutateladze correlation) and for turbulent regime (Chen correlation).

In order to prove the better thermal-hydraulic performance of a vertical tube condenser, a comparison between all the models has been provided through a simple Matlab code, taking as reference the SBWR IC mean tube data and considering the utilization of this condenser within the IRIS EHRS. A stratified flow is induced in case of horizontal tube, giving a pretty constant value of HTC (about 5500 W/m²K), except for tube end ($x < 0.1$) where condensate sump effects become dominant. The possibility of a slug-plug flow at low qualities is envisaged by Schaffrath’s analysis, making the condensation process in a horizontal tube a rather complex phenomenon, considered the risk of instabilities which could derive from intermittent flow regimes. Vertical tube film condensation theory, applied to the same set of data, shows that laminar wavy film condensation occurs only at tube entrance (up to a quality value of 0.95). The main process is governed by turbulent film condensation, which gives the dominant increasing trend of HTC with tube abscissa. Chen correlation predicts a mean HTC value of about 8000 W/m²K, rather higher when compared to the mean value of horizontal in-tube condensation.

Amongst the advanced LWR reactors adopting a vertical tube in-pool condenser for DHR applications, IRIS reactor is still in a conceptual design and pre-application phase. The better thermal-hydraulic behaviour of the vertical tube solution, stressed in the paper, can be intended as a scientific validation of the provided design choices.

Second goal of the work has been to validate the film condensation model for vertical tubes by means of experimental findings from PERSEO facility. Experimental HTC trend along tube abscissa has been reproduced for the SBWR IC tubes provided with wall thermocouples. The obtained results, in good agreement with the experimental work of Kim and No available in open literature, show an increasing HTC trend with tube abscissa, validating the proposed correlations and definitely confuting the Shah correlation under the particular conditions investigated.

As well as the commonly adopted Nusselt correlation for laminar film condensation, the two semi-empirical relationships proposed for laminar wavy regime (Kutateladze correlation) and turbulent regime (Chen correlation) appear preferable than any completely empirical relationship, as Shah correlation. This concern should be properly accounted when dealing with condensation phenomena, for example,

when a transient event on a nuclear reactor is simulated with a best-estimate thermal-hydraulic code. The implementation of the recommended heat transfer model is thus required for system codes like RELAP5, in which turbulent condensation is still dealt according to Shah correlation.

Appendix

This section describes how to apply the correlations presented for HTC evaluation dealing with condensation in a horizontal tube (Section 3.1) and in a vertical tube (Section 3.2), to predict condenser tube length required to accomplish the complete condensation of inlet steam.

Computational procedure, based on a subdivision of the pipe in many cells, is step-by-step shown in the followings.

Step 1. From the known thermal power to be exchanged and the chosen number of discretization intervals, evaluate the thermal power exchanged per cell W_{cell} :

$$W_{\text{cell}} = \frac{W}{N_{\text{cell}}}. \quad (\text{A.1})$$

Step 2. Calculate internal side (condensation) heat transfer coefficient h_{cond} , using one of the models/correlations proposed in the paper.

Step 3. Calculate external side (pool boiling) heat transfer coefficient h_{pool} , using one of the available correlations for a single tube submerged in a boiling pool, as the correlation due to Borishanski-Mostinsky [37], specifically valid for water:

$$h_{\text{pool}} = 0.10111 p_{\text{cr}}^{0.69} (1.8 p_r^{0.17} + 4 p_r^{1.2} + 10 p_r^{10}) \Phi^{0.7}. \quad (\text{A.2})$$

Step 4. Heat exchange process requires to be dealt considering every thermal resistance involved, representative respectively of internal side, tube metal side, external side, as well as fouling effects (both internal and external). Once each of these terms is known, calculate overall heat transfer coefficient as follows (internal surface is chosen as reference):

$$U_i = \left[\frac{1}{h_{\text{cond}}} + R_{f,i} + \frac{D_i \ln(D_e/D_i)}{2k_{\text{tube}}} + \frac{R_{f,e}}{D_e/D_i} + \frac{1}{h_{\text{pool}}(D_e/D_i)} \right]^{-1} \quad (\text{A.3})$$

Step 5. Evaluate heat transfer surface for each cell S_i :

$$S_i = \frac{W_{\text{cell}}}{U_i (T_{\text{sat},i} - T_{\text{sat},e})}. \quad (\text{A.4})$$

Step 6. Compute the length of each cell, and, by adding the differential lengths L' , compute tube total length L :

$$L' = \frac{S_i}{\pi D_i}, \quad (\text{A.5})$$

$$L = \sum L'.$$

Step 7. Evaluate local heat flux for each cell Φ' :

$$\Phi' = \frac{W_{\text{cell}}}{\pi D_i L'}. \quad (\text{A.6})$$

Step 8. Because of the dependence of pool boiling HTC on heat flux Φ , according to (A.2), an iterative procedure is required. The heat flux value obtained in Step 7 has to be considered for pool boiling HTC calculation in Step 3. Iterate from Step 3 to Step 7 until a check error on the resulting heat flux becomes smaller than a fixed value.

Acronyms

DHR:	Decay Heat Removal
ECT:	Emergency Cooldown Tank
EHR:	Emergency Heat Removal System
ESBWR:	European Simplified Boiling Water Reactor
GDCS:	Gravity Driven Cooling System
HTC:	Heat Transfer Coefficient
HX:	Heat eXchanger
IC:	Isolation Condenser
IRIS:	International Reactor Innovative and Secure
LOCA:	Loss Of Coolant Accident
KAERI:	Korea Atomic Energy Research Institute
KNGR:	Korea Next Generation Reactor
LWR:	Light Water Reactor
NOKO:	NOtKOndensator (emergency condenser)
NPP:	Nuclear Power Plant
PANDA:	PAssive Nachwarmeabfuhr- und DruckAbbau- testanlage (passive decay heat removal and depressurization test facility)
PCCS:	Passive Containment Cooling System
PERSEO:	in-Pool Energy Removal System for Emergency Operation
POLIMI:	POLItecnico di Milano (Polytechnic of Milan)
PRHRS:	Passive Residual Heat Removal System
PSI:	Paul Scherrer Institute
RPV:	Reactor Pressure Vessel
SBWR:	Simplified Boiling Water Reactor
SIET:	Societ Informazioni Esperienze Termoidrauliche (company for information on thermal-hydraulic experimentation)
SMART:	System integrated Modular Advanced Reactor
SWR1000:	Siede Wasser Reaktor–1000 MW _e (boiling water reactor – 1000 MW _e)
VISTA:	experimental Verification by Integral Simulation of Transient and Accidents

Nomenclature and Symbols

D :	Tube diameter (m)
f_i :	Interfacial roughness factor
G :	Mass flux (kg/(m ² s))

g :	Acceleration of gravity (m/s^2)
h :	Condensation heat transfer coefficient ($W/(m^2K)$)
h_c :	Convective condensation heat transfer coefficient ($W/(m^2K)$)
h_f :	Film condensation heat transfer coefficient ($W/(m^2K)$)
h_l :	Single-phase heat transfer coefficient (from Dittus-Boelter correlation) ($W/(m^2K)$)
j_D^* :	Dimensionless vapour velocity
k :	Thermal conductivity ($W/(mK)$)
L :	Tube length (m)
N_{cell} :	Number of tube discretization intervals
Nu_l :	Condensate Nusselt number
p_{cr} :	Critical pressure (bar)
p_r :	Reduced pressure (p/p_{cr})
Pr_l :	Condensate Prandtl number
R_f :	Fouling thermal resistance (m^2K/W)
Re_l :	Local condensate Reynolds number
Re_L :	Condensate Reynolds number evaluated at the end of the considered regime
S :	Heat transfer surface (m^2)
T :	Temperature (K)
U :	Overall heat transfer coefficient ($W/(m^2K)$)
W :	Exchanged thermal power (W)
x :	Thermodynamic equilibrium quality
α :	void fraction
Δh_{lg} :	Latent heat of vaporization (J/kg)
δ :	Film thickness of annular ring (horizontal tube) (m)
	Film thickness of condensate at the wall (vertical tube) (m)
Φ :	Heat flux (W/m^2)
Γ :	Mass flowrate (kg/s)
Γ_l :	Condensate mass flowrate (kg/s)
μ_l :	Liquid dynamic viscosity (Pa s)
ν_l :	Liquid kinematic viscosity (m^2/s)
θ :	Falling film stratification angle
ρ :	Density (kg/m^3).

Subscripts

cell:	Discretization interval
cond:	Condensation
e :	External
g :	Saturated steam
i :	Internal
l :	Saturated liquid
lam:	Laminar regime
lam_wavy:	Laminar wavy regime
pool:	pool boiling
sat:	Saturation
tube:	Tube metal
turb:	Turbulent regime
w :	wall.

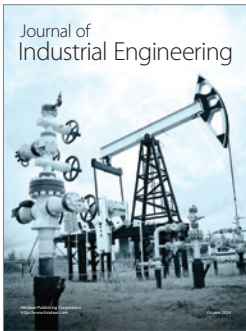
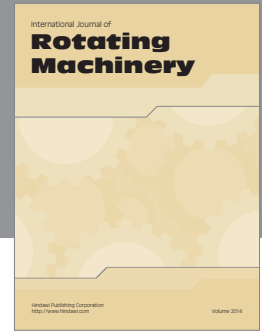
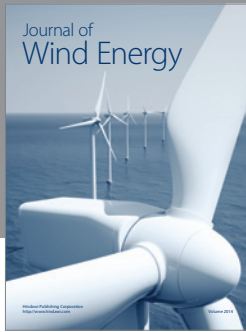
Acknowledgments

The authors wish to thank Fosco Bianchi (ENEA) for providing the experimental data from an integral test carried out during PERSEO project, and Roberta Ferri (SIET labs) for the deep and pleasant explanations on the facility behaviour. The authors are also grateful to the anonymous reviewers whose remarks have allowed significantly improving the paper organization and readability.

References

- [1] IAEA-TECDOC-626, "Safety related terms for advanced nuclear plants," September 1991.
- [2] R. Ferri, A. Achilli, G. Cattadori, F. Bianchi, and P. Meloni, "Design, experiments and Relap5 code calculations for the perseo facility," *Nuclear Engineering and Design*, vol. 235, no. 10-12, pp. 1201–1214, 2005.
- [3] A. Schaffrath, E. F. Hicken, H. Jaegers, and H.-M. Prasser, "Operation conditions of the emergency condenser of the SWR1000," *Nuclear Engineering and Design*, vol. 188, no. 3, pp. 303–318, 1999.
- [4] T. Sato and Y. Kojima, "Variations of a passive safety containment for a BWR with active and passive safety systems," *Nuclear Engineering and Design*, vol. 237, no. 1, pp. 74–86, 2007.
- [5] H. J. Kahn and U. S. Rohatgi, "Performance characterization of isolation condenser of SBWR," Tech. Rep. BNL-NUREG-47960, 1992.
- [6] S. J. Cho, B. S. Kim, M. G. Kang, and H. G. Kim, "The development of passive design features for the Korean Next Generation Reactor," *Nuclear Engineering and Design*, vol. 201, no. 2, pp. 259–271, 2000.
- [7] M. D. Carelli, L. E. Conway, L. Oriani, et al., "The design and safety features of the IRIS reactor," *Nuclear Engineering and Design*, vol. 230, no. 1-3, pp. 151–167, 2004.
- [8] Y.-J. Chung, H.-C. Kim, B.-D. Chung, M.-K. Chung, and S.-Q. Zee, "Two phase natural circulation and the heat transfer in the passive residual heat removal system of an integral type reactor," *Annals of Nuclear Energy*, vol. 33, no. 3, pp. 262–270, 2006.
- [9] H. Jaster and P. G. Kosky, "Condensation heat transfer in a mixed flow regime," *International Journal of Heat and Mass Transfer*, vol. 19, no. 1, pp. 95–99, 1976.
- [10] W. W. Akers, H. A. Deans, and O. K. Crosser, "Condensing heat transfer within horizontal tubes," *Chemical Engineering Progress Symposium Series*, vol. 55, pp. 171–176, 1959.
- [11] A. Cavallini and R. Zecchin, "High velocity condensation of organic refrigerants inside tubes," in *Proceedings of the 13th International Congress of Refrigeration*, vol. 2, pp. 193–200, Washington, DC, USA, August-September 1971.
- [12] M. K. Dobson and J. C. Chato, "Condensation in smooth horizontal tubes," *Journal of Heat Transfer*, vol. 120, no. 1, pp. 193–213, 1998.
- [13] J. El Hajal, J. R. Thome, and A. Cavallini, "Condensation in horizontal tubes—part 1: two-phase flow pattern map," *International Journal of Heat and Mass Transfer*, vol. 46, no. 18, pp. 3349–3363, 2003.
- [14] J. R. Thome, J. El Hajal, and A. Cavallini, "Condensation in horizontal tubes—part 2: new heat transfer model based on flow regimes," *International Journal of Heat and Mass Transfer*, vol. 46, no. 18, pp. 3365–3387, 2003.

- [15] J. R. Thome, "Condensation in plain horizontal tubes: recent advances in modelling of heat transfer to pure fluids and mixtures," *Journal of the Brazilian Society of Mechanical Sciences and Engineering*, vol. 27, no. 1, pp. 23–30, 2005.
- [16] F. P. Incropera, D. P. Dewitt, T. L. Bergman, and A. S. Lavine, *Fundamentals of Heat and Mass Transfer*, John Wiley & Sons, New York, NY, USA, 2007.
- [17] A. Schaffrath, A.-K. Krüssenberg, A. Fjodorow, U. Gocht, and W. Lischke, "Modeling of condensation in horizontal tubes," *Nuclear Engineering and Design*, vol. 204, no. 1-3, pp. 251–265, 2001.
- [18] T. N. Tandon, H. K. Varma, and C. P. Gupta, "A new flow regimes map for condensation inside horizontal tubes," *Journal of Heat Transfer*, vol. 104, no. 4, pp. 763–768, 1982.
- [19] H. M. Soliman, "The mist-annular transition during condensation and its influence on the heat transfer mechanism," *International Journal of Multiphase Flow*, vol. 12, no. 2, pp. 277–288, 1986.
- [20] P. G. Kosky and W. F. Staub, "Local condensing heat transfer coefficients in the annular flow regime," *AIChE Journal*, vol. 17, no. 5, pp. 1037–1043, 1971.
- [21] C. E. Rufer and S. P. Kezios, "Analysis of two-phase, one-component stratified flow with condensation," *Journal of Heat Transfer*, vol. 88, pp. 265–275, 1966.
- [22] G. Breber, J. W. Palen, and J. Taborek, "Prediction of horizontal tubeside condensation of pure components using flow regime criteria," *Journal of Heat Transfer*, vol. 102, no. 3, pp. 471–476, 1980.
- [23] L. E. Herranz, J. L. Muñoz-Cobo, and G. Verdú, "Heat transfer modeling in the vertical tubes of the passive containment cooling system of the simplified boiling water reactor," *Nuclear Engineering and Design*, vol. 178, no. 1, pp. 29–44, 1997.
- [24] S. Z. Kuhn, V. E. Schrock, and P. F. Peterson, "An investigation of condensation from steam-gas mixtures flowing downward inside a vertical tube," *Nuclear Engineering and Design*, vol. 177, no. 1–3, pp. 53–69, 1997.
- [25] H. C. No and H. S. Park, "Non-iterative condensation modeling for steam condensation with non-condensable gas in a vertical tube," *International Journal of Heat and Mass Transfer*, vol. 45, no. 4, pp. 845–854, 2001.
- [26] W. Nusselt, "The surface condensation of water vapour," *Zeitschrift des Vereins Deutscher Ingenieure*, vol. 60, pp. 541–546, 569–575, 1916.
- [27] S. S. Kutateladze, *Fundamentals of Heat Transfer*, Academic Press, New York, NY, USA, 1963.
- [28] D. A. Labuntsov, "Heat transfer in film condensation of pure steam on vertical surfaces and horizontal tubes," *Teploenergetika*, vol. 4, no. 7, pp. 72–79, 1957.
- [29] S. L. Chen, F. M. Gerner, and C. L. Tien, "General film condensation correlations," *Experimental Heat Transfer*, vol. 1, no. 2, pp. 93–107, 1987.
- [30] J. M. McNaught and D. Butterworth, "Film condensation of pure vapours," in *Heat Exchanger Design Handbook 2002*, vol. 2, Begell House, London, UK, 2002.
- [31] M. M. Shah, "A general correlation for heat transfer during film condensation inside pipes," *International Journal of Heat and Mass Transfer*, vol. 22, no. 4, pp. 547–556, 1979.
- [32] S. J. Kim and H. C. No, "Turbulent film condensation of high pressure steam in a vertical tube," *International Journal of Heat and Mass Transfer*, vol. 43, no. 21, pp. 4031–4042, 2000.
- [33] N. Aksan, "Overview on PANDA test facility and ISP-42 PANDA tests data base," in *Natural Circulation in Water Cooled Power Plants, IAEA-TECDOC-1474*, November 2005.
- [34] T. Bandurski, M. Huggenberger, J. Dreier, et al., "Influence of the distribution of noncondensibles on passive containment condenser performance in PANDA," *Nuclear Engineering and Design*, vol. 204, no. 1–3, pp. 285–298, 2001.
- [35] RELAP5/MOD3.3 Code, "Manual Volume IV: Models and Correlations," *NUREG/CR-5525 Rev 1*, 2001.
- [36] R. Ferri, A. Achilli, and S. Gandolfi, "PERSEO PROJECT: experimental data report," Tech. Rep. SIET 01 014 RP 02 Rev 1, 2003.
- [37] J. W. Palen, "Shell and tube reboilers," in *Heat Exchanger Design Handbook 2002*, vol. 3, Begell House, London, UK, 2002.



Hindawi

Submit your manuscripts at
<http://www.hindawi.com>

